phys. stat. sol. (a) **171**, 147 (1999)

Subject classification: 61.72.Cc; 61.72.Ji; 61.80.Fe; S.5.11

# Extended Defects Formation in Si Crystals by Clustering of Intrinsic Point Defects Studied by in-situ Electron Irradiation in an HREM

L. Fedina (a), A. Gutakovskii (a), A. Aseev (a), J. Van Landuyt (b), and J. Vanhellemont[1]) (c)

*(a) Institute of Semiconductor Physics, Russian Academy of Sciences, Pr. akad. Lavrentyeva 13, 630090 Novosibirsk, Russia*
*Fax: (3832)331080, e-mail: fedina@thermo.isp.nsc.ru*

*(b) University of Antwerp, RUCA EMAT, Groenenborgerlaan 171, B-2020 Antwerpen, Belgium*

*(c) IMEC, B-3001 Leuven, Belgium*

(Received October 5, 1998)

In situ irradiation experiments in a high resolution electron microscope JEOL-4000EX at room temperature resulted in discovery of the isolated and combined clustering of vacancies and self-interstitial atoms on {111}- and {113}-habit planes both leading to an extended defect formation in Si crystals. The type of the defect is strongly affected by the type of supersaturation of point defects depending on the crystal thickness during electron irradiation. Because of the existence of energy barriers against recombination of interstitials with the extended aggregates of vacancies, a large family of intermediate defect configurations (IDCs) is formed on {113}- and {111}-habit planes at a low temperature under interstitial supersaturation in addition to the well-known {113}-defects of interstitial type. The formation of metastable IDCs inside vacancy aggregates prevents a way of recombination of defects in extended shape.

## 1. Introduction

Few years ago the formation of extended defects in Si crystals via aggregation of self-interstitial atoms ($Si_i$) could be considered as well understood (for review of this topic, see [1]). This process has been studied in detail by in situ electron irradiation in a high voltage electron microscope (HVEM) at a wide temperature range between 20 and 1150 °C. Based upon clustering of very mobile $Si_i$ during electron irradiation, some of the coefficients of point defect reactions in Si (with dislocations, dopant atoms, and interfaces) have been determined [1]. An important conclusion is that the interaction coefficient of the less mobile vacancies with the real surface (or with surfaces capped with thin $SiO_2$ and $Si_3N_4$) is much larger than that for interaction with $Si_i$ (up to two orders of magnitude). The physical reason for this is not yet clear but the large vacancy capture coefficient of the surface results in an interstitial supersaturation close to the surface of Si specimens during irradiation. The supersaturated self-interstitials cluster in extended defects with preferably {113}-habit planes at relatively low irradiation temperature or they interact with dislocations at elevated temperatures. The interaction of

[1]) Present address: Wacker Siltronic AG, PO Box 1140, D-84479 Burghausen, Germany.

$Si_i$ with dislocations is related with the energy barrier of 1.3 eV for the transition of $Si_i$ from the metastable site in the core of dislocation to a stable lattice position in the plane of dislocation loop [1,2]. Because the displacement vectors of the {113}-defects do not correspond with the Burgers vectors of known dislocations, the concept of intermediate defect configurations (IDCs) was introduced by Tan in the early 1980s to interpret the experimental observation on the structure of extended aggregates of point defects occurring in crystals with diamond structure [3]. However, further detailed HREM studies of {113}-defects revealed a more complicated structure of the defect compared to the one predicted by Tan. Hexagonally arranged atomic rings followed by eight-membered ones in irregular succession in the plane of {113}-defect have been first revealed by Takeda in a high-resolution electron microscope (HREM) [4 to 6]. Similar results were obtained by Parisini and Bourret [7] based on ab initio calculations of the minimum energy of the defect. They have shown the appearance of large eight-membered O-rings inside the continuous hexagonal structure of {113}-defects leads to a decrease of the defect energy down to 0.6 eV per $Si_i$, i.e. to the formation of a relaxed atomic structure. But it was not clear whether O-rings were formed in the real structure by the disappearance of $Si_i$ away from the defect plane or not. On the contrary, the transformation of {113}-defects into perfect dislocation loops which is commonly formed during prolonged irradiation needs a complementary sink for $Si_i$ to the defect plane in order to fill up vacancy sites inside O-rings [5]. This contradiction disappears if one assumes that an irregular sequence of O-rings in an atomic structure of {113}-defects is created by accidental interactions of $Si_i$ with O-rings initially formed in the defect plane by the agglomeration of vacancies. This idea was not considered in the various models of the {113}-defect since defects of vacancy type on {113}-planes had never been detected in Si crystals. Recently, aggregates of vacancies on {111}-planes produced by electron irradiation in an HREM at room temperature have been revealed in very thin Si crystals where the sample forms also a sink for $Si_i$ [8 to 11]. It allowed the investigation of extended defect formation under vacancy supersaturation. We will show in the present paper that aggregation of vacancies on {113}-planes occurs during the initial stages of irradiation in this case, too. Furthermore, it is found that the structure of the vacancy aggregates is completely transformed by interaction with $Si_i$ in thicker parts of the Si specimens with an interstitial supersaturation [11 to 13]. In the following, we call this kind of interaction "combined clustering" of point defects. A fundamental reason of this phenomenon is the existence of energy and/or entropy barriers for transition of self-interstitial atoms from a metastable site (IDCs) to a stable lattice site. For instance in the plane of dislocation loop the barrier is about 1.3 eV [1,2]. We assume that the height of this barrier for combined clustering of point defects depends on the initial atomic structure of the vacancy agglomerate. This barrier can be considered, as well, as an energy barrier against recombination of point defects in extended shape proposed in [14]. The study of point defects aggregation in Si crystals during irradiation gives us a chance to understand the mechanism of secondary defect formation during crystal growth because both point defects and secondary defects become increasingly important as we march towards the era of Gbit devices [15].

The present paper provides a new look at the mechanisms of extended defect formation in Si depending on the type of supersaturation of point defects studied by in-situ electron irradiation in an HREM.

## 2. Experimental Details

Plan-view samples were prepared from wafers of high purity n-type FZ-Si with (110) orientation.[2]) Both surfaces of chemically thinned specimens were covered with 5 nm thick $Si_3N_4$ films by chemical vapor deposition in order to have a reproducible surface sink for intrinsic point defects created by electron irradiation [1]. In situ HREM experiments were carried out at room temperature in a JEM-4000EX microscope operated at 400 keV. The flux of electrons on a specimen during irradiation experiments was estimated to be about $10^{20}$ $cm^{-2}$ $s^{-1}$.

## 3. Results and Discussion

### *3.1 Extended defect formation in the very thin crystal*

Figs. 1a, b and c show typical HREM images of the extended aggregates of point defects on {111}-habit planes created during in situ HREM irradiation of very thin Si crystals (less than 10 nm). The distortion of {111}-planes parallel to the plane of separated defects shown in Figs. 1a, b indicates straightforwardly the vacancy sign of the defects, i.e. they are intrinsic Frank partial dislocation loops (FL). From the HREM image of the non-symmetrical V-shaped defect shown in Fig. 1c one can conclude that the image of one leg of the V-shaped defect differs from the other. Based upon the HREM image an atomic model of non-symmetrical V-shaped defect is presented in

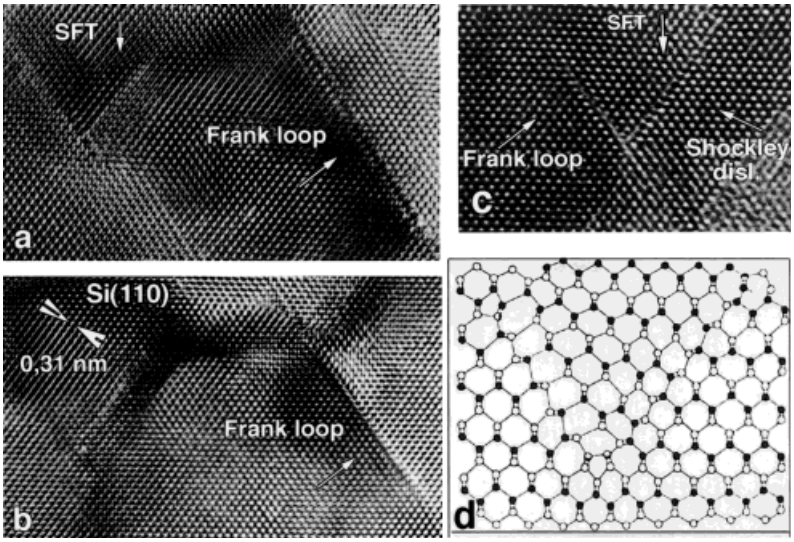


Fig. 1. a) to c) HREM images of the various defects of vacancy type in FZ-Si formed after 30 min of in-situ electron irradiation in very thin specimen areas (less than 10 nm): Isolated Frank loops and SFTs are marked. d) An atomic model of a non-symmetrical SFT based on the experimental HREM image

[2]) The FZ-Si crystals were grown by using a FZ-20 pulling machine in the framework of cooperation between the Institute of Semiconductor Physics (Novosibirsk) and 'Haldor Topsoe' A/S (Denmark).

Fig. 1d. The model reveals the correspondence of prismatic defect to FL and of non-prismatic defect to the Shockley dislocation gliding from the core or Frank dislocation. This defect seems to be a non-complete stacking fault tetrahedron (SFT). The other V-shaped defect shown in Fig. 1a has a symmetrical HREM image and is similar to the one found in Si crystals after phosphorous implantation [16]. Calculated HREM images of the V-shaped defects presented in [16] for both interstitial and vacancy type allowed to identify the symmetrical V-shaped defect in Fig. 1a as of vacancy type. The transformation of intrinsic FL into SFT in metals is known to be the classical relaxation of a defect with a high stacking fault energy. The energy of intrinsic stacking fault in Si is not known, but it seems to be also very high. Indeed, HREM images of FL in Figs. 1a, b reveal strong deformations around the defect planes even in the very thin foil where the stress can relax upon the top and bottom surfaces additionally to the gliding of Shockley dislocations. As a result the formation of non-complete SFT shown in Fig. 1c becomes possible as we assume to be the case.

Another type of extended defect found in the very thin irradiated area is presented in Fig. 2a. No visible distortion of {111}-planes crossing the defect plane is detected on the image of the defect which can be characterized by the sequence of small white dots located on a {113}-plane only. Because the HREM image was taken near the optimum defocus condition, every dark column on the image corresponds to the chain of atoms in [110] direction parallel to the electron beam. Therefore white dots arising at the place of dark columns located on {113} can be interpreted by the removal of atoms from the perfect atomic chain, in other words, by introducing of vacancies in the same direction. According to Tan's concept, vacancies (or divacancies) located in [110]-direction tend to form a continuous chain. This is a simple way of minimizing the defect energy, which is to minimize the number of broken bonds. From the model of the defect superimposed on the HREM image in Fig. 2b one can see that each of the small white dots on the defect plane is placed inside the O-ring. This means that each vacancy chain forms O-rings in (110) cross-section and no dangling bonds are involved

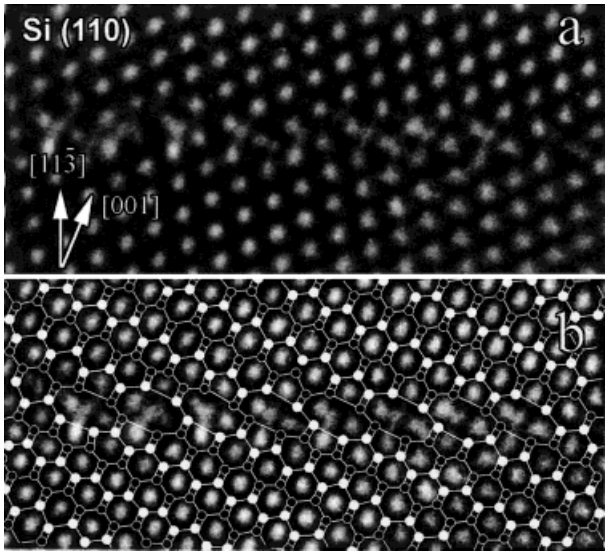


Fig. 2. a) [110] HREM image of a {113}-defect created after 20 min of in-situ electron irradiation in a very thin area of an FZ-Si crystal (less than 10 nm thick), b) the atomic model of the defect superimposed on the experimental image

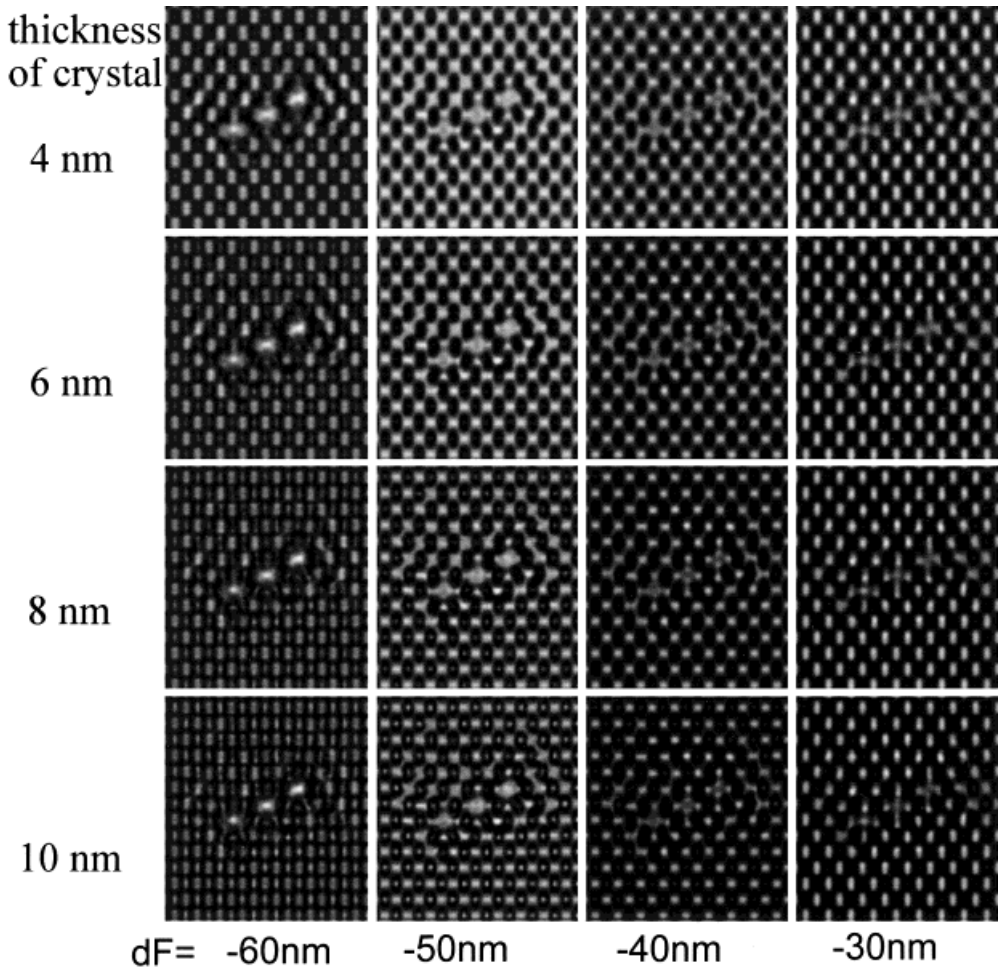


Fig. 3. Crystal thickness–defocus (dF) map of simulated images of a {113}-defect of vacancy type based upon the model shown in Fig. 2b

along the chain (excluding at its edges). Based upon this model, computer simulations of HREM images of {113}-defects consisting of three vacancy chains have been performed. The simulated images are presented in Fig. 3 in a through-focus series from −30 to −60 nm (underfocus) for an Si crystal with the thickness between 4 and 10 nm. From Fig. 3 one can see that the simulated images at defocus value dF = −30 nm reproduce well the characteristics of the experimental image in Fig. 2a in a whole thickness range. This allows for the conclusion that this defect is the extended {113}-defect of vacancy type consisting of vacancy chains located on {113}. Because there is no visible atomic column displacements around the {113}-defect, we also conclude that the one is characterized by a very small displacement vector within 0.01 to 0.02 nm. The defect is stable relatively to the transformation into other defects by means of the conservative process of glide that corresponds to its relaxed atomic structure. It agrees well with a small amount of calculated energy of a single vacancy chain (0.6 eV per vacancy) pre-

sented in [17]. The model of single vacancy chain being the same as used by us, was earlier predicted by Tan as the initial stage of intrinsic 90° dislocation dipole formation gliding on {100}-habit plane [3]. In our experiments, however, we could not observe the transformation of vacancy chains into dipoles but rather the formation of extended aggregates of vacancies on {113}. Therefore, this defect is a new type of extended defect in Si crystal with a smallest displacement vector originating from aggregation of vacancies in the shape of chains.

### *3.2 The extended defect formation in thicker crystal parts*

Only about 10% of the defects found in the part of irradiated crystal thicker than 10 nm consist of defects in {111}-planes, whereas {113}-defects are the dominant defect type [13]. Figs. 4a and b present the sequential formation stages of the same point defects aggregate on the {111}-plane formed, respectively, after 25 and 35 min of electron irradiation in an HREM. The defect is characterized in its initial stage by a visible distortion of {111}-planes parallel to the plane of the defect, which has the vacancy sign (see Fig. 4a). This defect is considered as a small FL partly filled with $Si_i$. For more details of the defect in this stage we refer to [13]. Further electron irradiation leads to complete transformation of FL into a {111}-defect yielding a HREM-image without any measurable distortion of the {111}-planes parallel to the defect plane in Fig. 4b. The model of the {111}-defect (Fig. 5a) deduced from the experimental HREM image reveals, in this stage, a regular sequence of double five-membered and single O-rings in the defect plane viewed in (110) cross-section. Interstitial chains (double $Si_i$ in the model in Fig. 5a) inserted in the plane of FL compensate for its displacement vector, but the perfect crystal structure is not fully restored. Based upon the unit cell used for the calculation shown in Fig. 5a, the simulated HREM image of the {111}-defect is presented in Fig. 5c. Differences between the calculated (Fig. 5c) and experimental (Fig. 5b) HREM images are probably due to the low relaxation rate of silicon bonds at room temperature in the disturbed area. This means that the positions of $Si_i$ in the

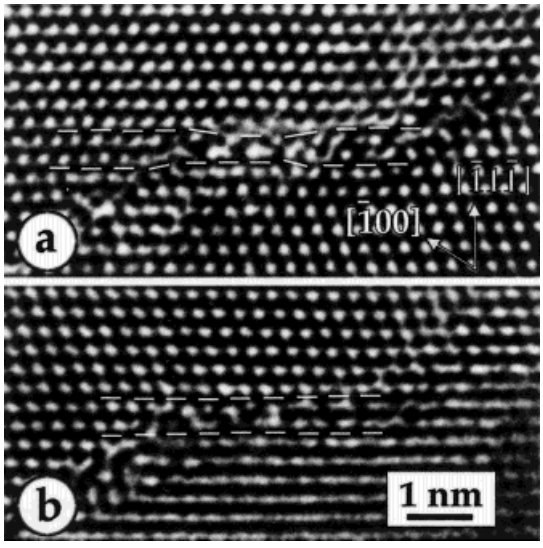


Fig. 4. HREM images of one and the same {111}-defect after a) 25 min and b) 35 min of electron irradiation in the high-resolution electron microscope

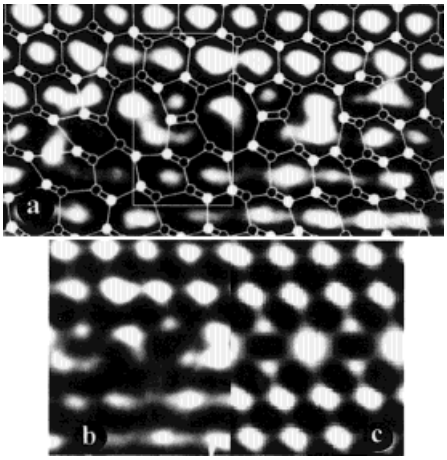


Fig. 5. a) An atomic model of the {111}-defect superimposed on the experimental HREM image of the defect in a final stage (cf. Fig. 4b). b) The central part of the experimental image in comparison with c) the calculated one made on the basis of the atomic model as drawn in a)

interstitial chain may be slightly misoriented from the [110]-direction. It is clear that the insertion of $Si_i$ in the plane of the vacancy loop provides its relaxation. Using the equation of Baraff et al. [18] and Nandedkar et al. [17], the energy of the {111}-defect can be determined in dependence on the amount of the force constant to be within the range of 0.34 to 1.10 eV per $Si_i$. The last value of the defect energy is close to the one calculated by Chou et al. for {111}-defects produced by ion implantation [19]. The small energies of the {111}-defect strongly suggest its higher stability compared to the initial vacancy loop. Thus, the relaxation of FL can be realized by interaction with interstitials, too. The atomic structure of the {111}-defects results from new IDCs which are formed on {111}-planes by insertion of $Si_i$ to the core of both vacancy and interstitial Frank partial dislocation loops during irradiation at relatively low temperature [11 to 13]. The existence of an energy barrier of 1.3 eV for the transition of $Si_i$ from IDCs to stable lattice positions in the plane of FL prevents the recombination of $Si_i$ with the vacancy loop at room temperature, but at higher temperature they will recombine.

Figs. 6a to d show the experimental HREM images of the same aggregates of point defects on {113}-plane after 25 and 35 min of irradiation, respectively (a and b), with the atomic models superimposed on the images (c and d). The model of the defects in their initial stage (Fig. 6c) reveals the formation of a three-dimensional cluster consisting of two parallel {113}-defects connected with each other by the sequence of five-membered atomic rings. From comparison of the HREM image of {113}-defect at the bottom in Fig. 6a with the simulated images in Fig. 3 we conclude that the large white spots in the defect plane corresponding to vacancy chains are formed at defocus value $dF = -60$ nm. The shape and brightness of the white spots in the plane of the {113}-defect have to depend strongly on the number of vacancies in the chains as well as on the amount of inward relaxation of the vacancy chain, i.e. on the deformation of O-rings as we assume. The small white dots in the plane of the upper {113}-defect in Fig. 6a appear to be rather due to the deformation of O-rings in [001]-direction (see Fig. 6b). Much more calculation and experimental work remains to be done in order to elucidate in detail the structure of large aggregates of vacancies. Anyway, the experimental HREM image of the bottom {113}-defect in Fig. 6a can be interpreted as an aggregate consisting of chains of vacancies on a {113}-plane. The structure of the defect

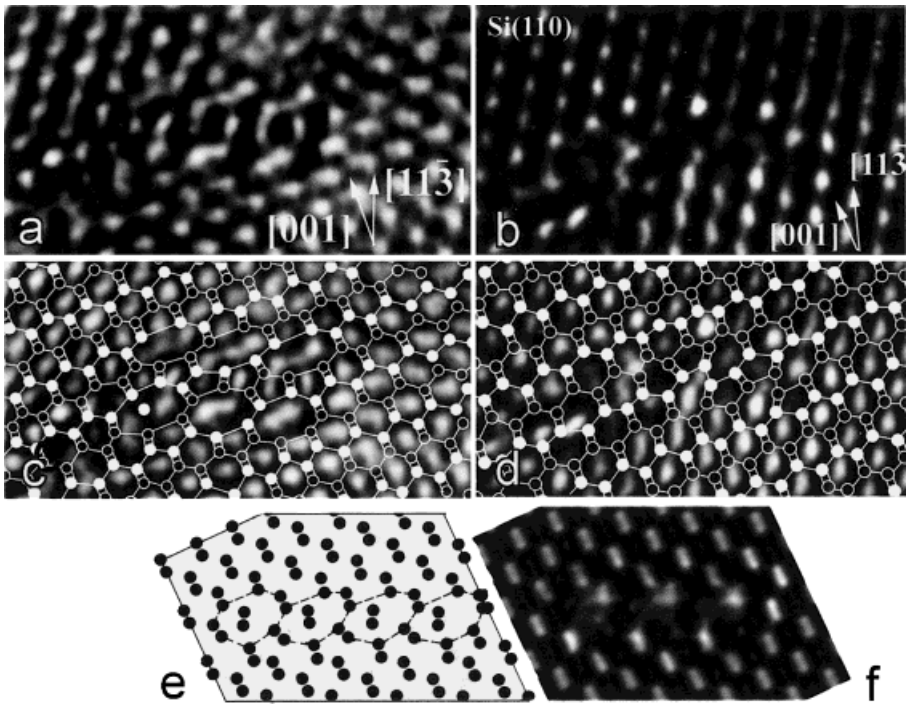


Fig. 6. HREM images of one and the same {113}-defect after a) 25 min and b) 35 min of electron irradiation. c), d) Corresponding structural models superimposed on the experimental images. e) Geometric atomic model of {113}-defect in a further formation stage obtained by insertion of double self-interstitials inside initially formed eight-membered rings shown with broken lines. f) Computer simulated image of a {113}-defect based on the model presented in e). Parameters for the calculation: defocus value dF = −60 nm and specimen thickness 15 nm

is dramatically changed during further irradiation (Fig. 6b) and a short sequence of double five- and double seven-membered atomic rings can be found on the atomic model of the defect superimposed on the image (Fig. 6d). The same model can be easily designed by geometrical modeling of O-rings on the {113}-plane followed by further insertion of double $Si_i$ (interstitial chain) inside each of the O-rings and rearrangement of the Si–Si bonds in the defect plane (Fig. 6e). Based upon this model the simulated HREM image presented in Fig. 6f is in satisfactory agreement with the experimental one in Fig. 6b. This is because the real chain structure in the [110]-direction is changed during irradiation which was not taken into account in the simulation. Clearly, this kind of {113}-defect is very metastable. The model of {113}-defect in this stage is close to that one of interstitial type predicted by Tan [3]; however, this defect is not of interstitial nor of vacancy type. It is a so-called "zero"-defect, since a small rotation of the interstitial chain inside the O-ring and an additional rearrangement of Si–Si bonds lead to the restoration of a perfect crystal structure, i.e. to recombination of the vacancy chain. The recombination is controlled rather by the rate of rearrangement of Si–Si bonds inside the vacancy chain. Taking into account the high energy of this kind of IDCs for interstitial type {113}-defects in Tan's model (5.4 to 8.7 $J/m^2$) obtained by tight-binding calculation [20], we may assume that the energy of the "zero" {113}-defect

has to be also high enough, but not higher than 1.3 eV for transition of $Si_i$ from IDCs to stable lattice positions in the plane of the dislocation loops [1,2]. Surprisingly, the interaction of $Si_i$ with initially stable aggregates of vacancies on {113}-planes having small energy (0.6 eV per vacancy, [17]) leads to the formation of metastable {113}-defects with higher energy. This is possible if it reduces the energy of isolated $Si_i$ (5 to 6 eV per $Si_i$, [21]) as well as the total energy of the system in general. On the other hand, it evidences the existence of an energy barrier against recombination of point defects in extended shape as predicted in [14]. It is clear that the formation of metastable IDCs inside a vacancy aggregate prevents recombination of the defects in extended shape. We have to notice that it is true only for interaction of mobile $Si_i$ with an extended aggregate of vacancies under interstitial supersaturation. There is no detectable energy barrier for interaction of mobile vacancies with an extended aggregate of interstitials in the shape of IDCs, which always tend to disappear during irradiation at high intensity of the electron beam [1,11,13].

Another typical example of the transformation of a point defects aggregate on a {113}-habit plane during irradiation at room temperature is presented in Fig. 7. The HREM images in Figs. 7a, b reveal a very disturbed structure of the {113}-defect in its

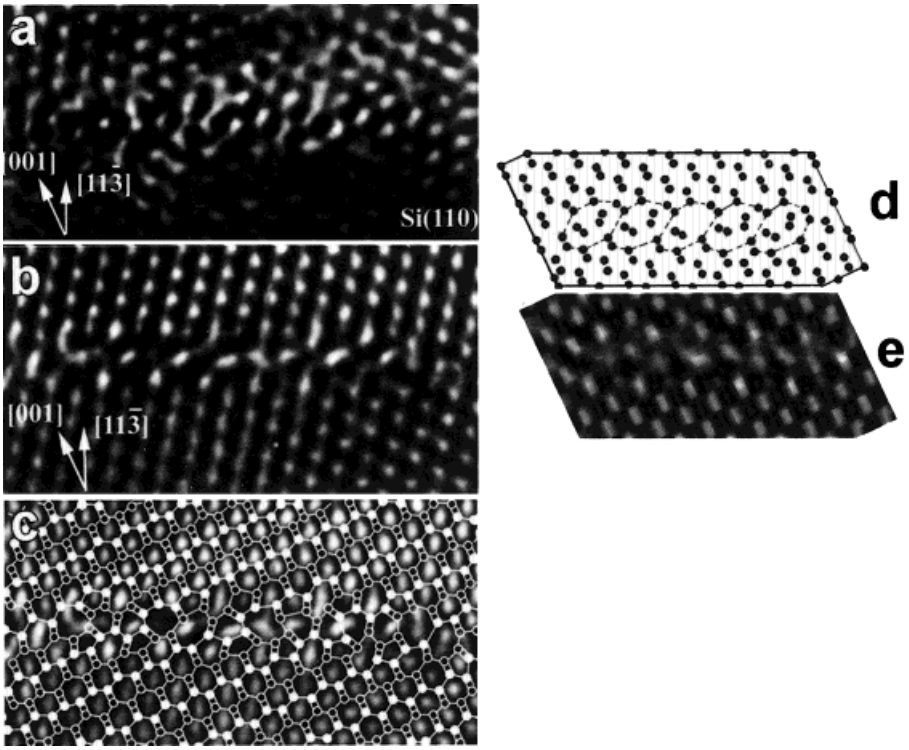


Fig. 7. HREM images of one and the same {113}-defect in a) initial and b) final formation stages after 25 and 35 min of irradiation, respectively. Atomic models of the {113}-defect in the final stage c) as superimposed on experimental image and d) as constructed by inserting of four interstitials inside some of the O-rings shown with broken lines. e) Simulated HREM image of a {113}-defect obtained by use of model d). Parameters for the calculation: defocus value dF = −60 nm and specimen thickness 15 nm

initial stage (a) and a more regular structure with a pronounced {113}-habit plane in its final stage (b). The atomic model of the defect in the final stage superimposed on the HREM image in Fig. 7c includes strongly deformed hexagonally arranged six-membered atomic rings followed by O-rings in irregular succession on the defect plane. This type of structure can be build up on the basis of the model of the "zero" {113}-defect with additional insertion of $Si_i$ on the defect plane. Two interstitial chains have to be inserted inside some of the O-rings to create the irregular hexagonal structure as shown in Fig. 7d. The simulated HREM image of the {113}-defect obtained by using this model and shown in Fig. 7e is in satisfactory agreement with the experimental one (Fig. 7b). Both atomic models of the defect in Figs. 7c, d are similar to that one proposed by Takeda [4,5] for relaxed interstitial type {113}-defects produced by HVEM electron irradiation at 400 °C. The energy of the relaxed {113}-defect varies in a range between 0.6 and 1.12 eV per $Si_i$ in dependence on the arrangement of hexagonal six-membered rings and O-rings on {113}-plane [7,22]. The energy of the non-relaxed {113}-defect of interstitial type shown in Fig. 7b has to be smaller than the energy of the "zero" {113}-defect, too (see Fig. 6b). In this case the time of recombination of point defects will be larger than the one for insertion of other mobile $Si_i$ into the vacancy agglomerate and the formation of a {113}-defect of interstitial type becomes possible. In fact, the fast accumulation of $Si_i$ inside a vacancy aggregate provides the formation of an amorphous-like structure of {113}-defects during the initial stage of aggregation of point defects on {113}-planes which are further transformed to hexagonal structure. The formation of an amorphous-like structure of {113}-defects giving an amorphous diffraction pattern in HVEM irradiation experiments at a temperature range between 20 and 300 °C has been reported [11].

## 4. Conclusion

The results obtained clearly evidence that the type of extended defect generated in a Si crystal during electron irradiation in a HREM at room temperature is strongly affected by the type of point defect which is present in supersaturation, and depends strongly on specimen thickness and the surface type. Because of the very limited sink of self-interstitials at the surface, a vacancy supersaturation is realized in the very thin part of Si crystals (less than 10 nm) only, while an interstitial supersaturation dominates in the thicker parts. It is found that vacancies cluster in the shape of extended defects in both {111}- and {113}-planes, which are totally different regarding their structure and the initial lattice relaxation around defect planes (displacement vectors). Strongly stressed two-dimensional aggregates of vacancies on {111} relax upon gliding of Shockley dislocations under vacancy supersaturation or upon interaction with interstitial atoms under interstitial supersaturation. On the contrary, the weakly strained one-dimensional vacancy chains located on {113} are stable under vacancy supersaturation, but they become the traps of interstitials under interstitial supersaturation. Our results confirm Tan's concept of IDC formation in general and provide some new insights into point defect clustering on {113}-habit planes in case of a supersaturation of both types of intrinsic point defects. The high probability of agglomeration of vacancies on {113}-planes with a low-energy barrier seems to be the main reason for further clustering of self-interstitials on {113}-planes resulting in the formation of IDCs with low energy per interstitial atom or in the recombination of intrinsic point defects.

***Acknowledgements*** This work was supported by grant No. 98-02-11798 from the Russian Foundation of Basic Research. L. F. is grateful to the Belgian Science Policy Office (DWTC) for her fellowship at RUCA EMAT (Antwerp).

## References

[1] A.L. Aseev, L.I. Fedina, D. Hoehl, and H. Bartsch, Clusters of Interstitial Atoms in Silicon and Germanium, Akademie Verlag, Berlin 1994 (p. 152).
[2] L. Fedina and A.L. Aseev, phys. stat. sol. (a) **95**, 517 (1986).
[3] T.Y. Tan, Phil. Mag. A **44**, 101 (1981).
[4] S. Takeda, Jpn. J. Appl. Phys. **30**, L639 (1991).
[5] S. Takeda, M. Kohyama, and K. Ibe, Phil. Mag. A **4**, 287 (1994).
[6] J.L. Hutchison, A.L. Aseev, and L.I. Fedina, Inst. Phys. Conf. Ser. **134**, Sect. 1, 41 (1993).
[7] A. Parisini and A. Bourret, Phil. Mag. A **67**, 605 (1993).
[8] S. Takeda and S. Horiuchi, Ultramicroscopy **54**, 144 (1994).
[9] L. Fedina, J. Van Landuyt, J. Vanhellemont, and A. Aseev, Mater. Res. Soc. Symp. Proc. **404**, 189 (1996).
[10] L. Fedina, J. Van Landuyt, J. Vanhellemont, and A. Aseev, Nuclear. Instrum. and Methods **B112**, 133 (1995).
[11] L. Fedina, A. Gutakovskii, A. Aseev, J. Van Landuyt, and J. Vanhellemont, in: In situ Electron Microscopy in Material Research, Kluwer Internat. Academic Publ., Dordrecht 1997 (p. 63).
[12] L. Fedina, A. Gutakovskii, A. Aseev, J. Van Landuyt, and J. Vanhellemont, Inst. Phys. Conf. Ser. **157**, 43 (1997).
[13] L. Fedina, A. Gutakovskii, A. Aseev, J. Van Landuyt, and J. Vanhellemont, Phil. Mag. A **77**, 423 (1998).
[14] U. Gösele and T.Y. Tan, in: Diffusion in Solids. Unsolved Problems, TransTech Publ., Zürich 1992 (p. 189).
[15] Kyong-Min Kim, Solid State Technology, November 1996, p. 70.
[16] W. Coene, H. Bender, and S. Amelinckx, Phil. Mag. A **52**, 369 (1985).
[17] A.S. Nandedkar and J. Narayan, Phil. Mag. A **56**, 625 (1987).
[18] G.A. Baraff, E.O. Kane, and M. Schluter, Phys. Rev. B **21**, 5662 (1980).
[19] C.T. Chou, D.J.H. Cockayne, J. Zou, P. Kringhoj, and C. Jagadish, Phys. Rev. B **52**, 17223 (1995).
[20] K. Masuda and K. Kojima, J. Phys. Soc. Japan **52**, 10 (1983).
[21] W.H. Press, B.P. Flannery, S.A. Teukolsky, and W.T. Vettering, Numerical Recipes, Cambridge University Press, Cambridge 1986 (p. 131).
[22] M. Kohyama and S. Takeda, Phys. Rev. B **46**, 12305 (1992).